THE ASTROPHYSICAL JOURNAL, 346:265–276, 1989 November 1

A STUDY OF SEVERAL F AND G SUPERGIANT-LIKE STARS WITH INFRARED EXCESSES AS CANDIDATES FOR PROTO–PLANETARY NEBULAE

BRUCE J. HRIVNAK[1]
Department of Physics, Valparaiso University
SUN KWOK
Department of Physics, The University of Calgary
AND
KEVIN M. VOLK
NASA Ames Research Center
Received 1988 October 6; accepted 1989 April 29

ABSTRACT

Ground-based observations have been obtained for eight F and G supergiant-like stars showing large infrared excesses. The combination of ground-based and *IRAS* data shows that these objects have dual-peak energy distributions, with comparable amounts of energy emitted in the visible and the infrared. The infrared-emitting cool dust shells are likely to represent the remnants of ejecta from an earlier phase of evolution. It is suggested that these eight objects are similar to IRAS 18095+2704 and are intermediate-mass stars in a post–asymptotic giant branch (AGB) phase of evolution. Model fittings to the 0.4–100 μm energy distribution of these objects suggest that they left the AGB within the last 1000 yr.

Subject headings: infrared: sources — nebulae: planetary — stars: circumstellar shells — stars: supergiants

I. INTRODUCTION

It has been suggested recently that a number of high-latitude F supergiants, the so-called 89 Her objects, are actually old, halo objects observed in the post–asymptotic giant branch (post–AGB) phase (Bond, Carney, and Grauer 1984). Among the properties exhibited by various members of this class (but not by all) are high space velocity, low metal abundance (Bond and Luck 1987), circumstellar dust (Parthasarathy and Pottasch 1986), and molecular envelopes (Likkel *et al.* 1987). These observational data are consistent with the interpretation that these are low-mass objects which have lost their envelope mass and are now in a post–AGB phase. Although the list of such objects based upon optical characteristics may actually contain a rather diverse group of objects, some of these we believe to be proto–planetary nebulae (PPN) candidates, as we will discuss later in this paper.

While the high latitude of the objects drew attention to them optically, one would expect to find low-latitude counterparts which are also post-AGB objects, although not necessarily metal poor. These would be harder to distinguish optically. However, by searching the *IRAS* sky survey data, the opportunity exists to first identify candidate objects based upon their infrared emission due to a dust shell, and then to see if optical counterparts exist. This is how we proceeded in the present study.

Examples of objects which have been previously identified as post–AGB based upon their infrared excesses are HD 161796 (IRAS 17436+5003) and HD 101584 (IRAS 11385−5517) by Parthasarathy and Pottasch (1986), HR 4049 (IRAS 10158−2844) by Lamers *et al.* (1986), IRAS 20051+1823 by Menzies and Whitelock (1988), and IRAS 18095+2704 by Hrivnak, Kwok, and Volk (1988). For the last of these, the source was selected on the basis of its peculiar spectrum as observed by the *IRAS* low resolution spectrometer (LRS; Volk and Kwok 1987) and was subsequently identified with a 10th mag F3 Ib star. The simultaneous presence of a 7000 K photospheric continuum and $\approx$150 K dust component was interpreted as resulting from a low-mass star evolving across the H-R diagram on the way to become a planetary nebula, with starlight emerging out of the fossil dust shell ejected during the AGB phase.

Another post–AGB object is IRC +10420 (IRAS 19244+1115), a strong infrared and OH source which has been the subject of many studies, and which we will discuss below. Evidence for its post–AGB and possible PPN nature is given by Fix and Cobb (1987).

We define the proto–planetary nebula phase in the following way. Stars on the AGB are known to be losing mass at a high rate, and if the initial mass is large enough, their photospheres may become totally obscured. These objects can, however, be observed at infrared wavelengths. When the mass loss reduces the envelope mass below a certain value, the star will begin to evolve toward the blue side of the H-R diagram. When the envelope mass is reduced to a still lower value, large-scale mass loss ends, and we designate this point as the beginning of the PPN phase (see Kwok 1987). During this phase, the inner shell radius increases, the dust shell temperature decreases, and the temperature of the central star increases. When the central star is hot enough to ionize the circumstellar nebula, the PPN phase ends and the object is now classified as a planetary nebula. The duration of the PPN phase is expected to last up to several thousand years (Schönberner 1983).

In this paper we report the identification of eight *IRAS* sources which exhibit the spectra of types F and G, and in one case late-A, supergiants, found at a variety of galactic latitudes, which we believe to be in a post–AGB phase of evolution, and which appear to be good candidates for PPN. We discuss their observational properties and analyze their flux distributions with a dust radiative transfer model applied to a detached

[1] Visiting Astronomer at the Dominion Astrophysical Observatory, National Research Council of Canada.

TABLE 1

CANDIDATES FOR PROTO–PLANETARY NEBULAE

IDENTIFICATIONS						GALACTIC COORDINATES	
IRAS	SAO	HD	DM	RAFGL	Other	l	b
07134+1005	96709	56126	+10 1470	...	...	206.7	+10.0
10215−5916	...	...	−58 3221	4106	CPD-58 2154	285.1	−1.9
12175−5338	239853	...	−53 4543	...	CPD-53 5072	298.3	+8.7
17436+5003	30548	161796	+50 2457	5384	V814 Her	77.1	+30.9
19114+0002	124414	179821	−00 3679	2343	...	35.6	−5.0
19244+1115	...	...	...	2390	IRC +10420	47.1	−2.5
19500−1709	163075	187885	−17 5779	...	...	24.0	−21.0
20004+2955	...	...	+29 3865	...	V1027 Cyg	67.4	−0.4

envelope. The fit of the model to the observations of each object is discussed, and the argument made that these objects possess the expected properties of proto–planetary nebulae, particularly that of a well-detached, cool dust shell. A quantitative comparison of the derived properties of these PPN candidates is then made.

II. CANDIDATES FOR PROTO–PLANETARY NEBULAE

The PPN candidates in this study were selected based upon either the shape of the LRS spectrum, their previous suggestion as a PPN candidate, or their location in the *IRAS* color-color plane ([25/12] vs. [60/25]). For the last criterion, a region of the plane was defined which contained previously identified PPN candidates and known young, compact planetary nebulae, but which excluded M stars with circumstellar dust shells. From this region additional color-selected candidates were identified. More details of this selection can be found in Volk and Kwok (1989).

In Table 1 are listed the objects of the present study. For uniformity, we will refer to the objects by their *IRAS* identifications. Additional identifications are listed in Table 1. The association of the *IRAS* source with the optical counterpart is based upon a close positional association, and in some cases the agreement with previous ground-based infrared observations. It would be desirable to confirm the association of each of these directly by flux measurements at 10 μm, as was done for IRAS 18095+2704. However, only in the association of RAFGL 4106 with IRAS 10215−5916 is there any significant difference between the *IRAS* and ground-based positions, and in this one case the ground-based data confirm the identification. Thus we believe that there is no reason to doubt the correctness of any of these associations.

Recently Odenwald (1986) searched the *IRAS* Point Source Catalog for associations of *IRAS* sources and G-type stars. He found that of the 150 G supergiants detected by *IRAS*, excess emission was found in $\approx$4%. Two of his infrared excess objects are in common with this study. Several of the supergiants which he identified are RV Tauri variables, which have long been known to possess infrared excesses at 10 μm (Gehrz 1972). The evolutionary status of RV Tauri stars as post–AGB objects of low mass has been discussed recently by Jura (1986). None of the sources in the present study has been classified as RV Tauri variables.

IRAS data for each of these eight sources are listed in Table 2. The *IRAS* broad-band measurements have been taken from the second edition of the *IRAS* Point Source Catalog, and have been color-corrected using the procedure described in Kwok, Hrivnak, and Milone (1986). The energy distributions of most of the objects peak around 20–30 μm. Five of the sources have infrared spectra listed in the Atlas of Low Resolution *IRAS* Spectra (LSRC; *IRAS* Science Team 1986). Two of these are characterized as class 05, which indicates a low signal-to-noise red spectrum. Two others are classified as class 66 and 69, which indicate the 10 μm silicate feature in emission on a red continuum. One object is classified as class 28, implying a strong silicate emission feature on a blue continuum. Spectra for the other three were extracted from the LRS data bank supplied by the Space Research Laboratory at the University of Groningen. The probability of variability of each object is also listed in Table 2, as given in the *IRAS* Point Source Catalog. They are all assigned a low probability of variability, $<$50%.

Pottasch and Parathasarathy (1988) recently identified several F and G giants and supergiants which display infrared excesses, including two objects in common with this study—IRAS 19114+0002 and IRAS 19500−1709. Their analysis, however, did not include the addition of non–*IRAS* photometric data, as have been incorporated into this study.

TABLE 2

IRAS MEASUREMENTS

	COLOR-CORRECTED FLUXES (Jy)					
IRAS ID	12 μm	25 μm	60 μm	100 μm	LRS	VAR(%)
07134+1005	29.5	112.8	40.5	14.1	...	0
10215−5916	233.3	1763.0	685.0	166.1	66	6
12175−5338	1.1	20.3	6.0	2.3	...	5
17436+5003	6.1	202.2	125.3	44.7	05	35
19114+0002	33.0	702.9	424.8	154.1	...	4
19244+1115	1582.0	2028.0	564.3	170.6	28	0
19500−1709	33.2	161.2	58.8	16.7	05	3
20004+2955	35.3	29.0	3.5	$<$33.5	69	15

III. OBSERVATIONAL PROPERTIES

a) *New Observations*

For almost all of the objects in this study, new ground-based optical photometry and spectroscopy, and infrared photometry were obtained at a variety of observatories. The new photometry is listed in Table 3, along with the date (UT) and the name of the associated observatory.

New optical *UBV* photometry was obtained for four of the sources using the 0.6 m telescope at Yerkes Observatory. We made the observations under fair conditions for all-sky photometry, and the data were transformed to the Johnson system through the use of standard stars observed nightly. For two of the southernmost objects (IRAS 10215−5916 and 12175−5338), *UBVRI* photometry was obtained by D. Geisler at Cerro Tololo Inter-American Observatory (CTIO) with the 1.0 m telescope. The *UBV* observations were on the Johnson system, and *RI* on the Cousins system.

New near-infrared observations were obtained at three sites. At Kitt Peak National Observatory (KPNO), R. Joyce observed four of the northern sources at *JHKLM* bandpasses. The 1.3 m telescope was used, with the BT InSb photometer, a 15″ aperture, and a throw of 40″ north-south, except when source confusion was obvious on the television monitor. At the South African Astronomical Observatory (SAAO), P. Whitelock observed the four southernmost sources at *JHKL* bandpasses with the 0.75 m and 1.9 m telescopes. At the United Kingdom Infrared Telescope (UKIRT), *JHKL'M* photometry was obtained by the resident astronomers for two objects using the UK9 InSb photometer. Apertures of 8″ and 12″ were used. The *M* filters at KPNO and UKIRT are narrow-band filters.

Mid-infrared observations were obtained at UKIRT for IRAS 07134+1005. The observations were carried out by resident astronomers using the UK8 bolometer. A 6″ aperture was used in the observations. Standard stars at similar airmasses and average extinction coefficients were used in the reduction of all the UKIRT observations.

Optical spectra of five of the objects were obtained at the Dominion Astrophysical Observatory (DAO), with an intensified Reticon detector. They were all observed with the 1.2 m coudé system, at a reciprocal dispersion of 20 Å mm^{-1} and a resolution of ≈ 1.5 Å. Approximate spectral types were determined by comparison with a few spectral standards observed with the same instrumentation, and by reference to the photographic spectral atlas by Yamashita, Nariai, and Norimoto (1978). The derived spectral classifications are listed in Table 3, and they all appear to be in accord with the published classifications based upon lower dispersion studies and listed below. We have displayed for future reference these spectra in Figure 1 along with some spectral standards. IRAS 18095+2704 is also included for comparison. The spectra have not been flux-calibrated. These objects should be studied for spectral variations over the next several decades. The five objects were observed in 1988 April and May; a few earlier spectra were also obtained in 1987 August with the DAO 1.8 m Cassegrain telescope. Multiple radial velocity observations of four of these sources have been made at DAO, using the 1.2 m telescope and radial velocity spectrometer to obtain high-precision velocities.

TABLE 3

NEW GROUND-BASED OBSERVATIONS

A. Visible

IRAS ID	Date	*U*	*B*	*V*	R_c	I_c	Observatory	Spectral Type
07134+1005	...	...	...	...	...	...	...	F0–5 I–Ia
10215−5916	1988 Mar 18	11.22	10.24	8.73	7.68	6.54	CTIO	...
12175−5338	1988 Mar 18	10.15	9.68	9.30	9.05	8.78	CTIO	...
17436+5003	1987 Sep 04	7.84	7.42	7.00	...	...	Yerkes	F2–5 Ib
19114+0002	1987 Sep 04	10.81	9.49	7.89	...	...	Yerkes	~G5 Ia
19500−1709	1987 Sep 04	9.34	9.19	8.67	...	...	Yerkes	F2–6 Ia
20004+2955	1987 Sep 04	13.3	11.28	8.94	...	...	Yerkes	~G7 Iab

B. Infrared

IRAS ID	Date	*J*	*H*	*K*	*L*	*L'*	*M*	Observatory
07134+1005	1987 Oct 06	6.84	6.57	6.59	6.43	...	5.86[a]	KPNO
	1988 Apr 06	7.00	6.76	6.70	...	6.49	6.29[b]	UKIRT
10215−5916	1987 Nov 20	4.61	3.49	3.02	2.58	...	...	SAAO (0.75 m)
12175−5338	1987 Nov 19	8.47	8.25	8.15	...	...	...	SAAO (0.75 m)
	1988 Mar 31	8.41	8.23	8.13	8.03	...	...	SAAO (1.9 m)
19114+0002	1988 Mar 31	5.01	4.52	4.27	4.05	...	...	SAAO (1.9 m)
	1988 Apr 10	4.98	4.51	4.28	...	4.00	3.71	UKIRT
19500−1709	1987 Oct 07	7.20	6.94	7.04	6.60	...	6.14[a]	KPNO
	1988 Mar 31	7.16	6.90	6.77	6.54	...	...	SAAO (1.9 m)
20004+2955	1987 Oct 07	4.79	4.15	4.01	3.38	...	3.06	KPNO
		$\lambda(\mu m)$	8.75	9.7	10.5	11.5	12.5	19.5
IRAS ID	Date	$\Delta\lambda(\mu m)$	1.2	...	1.0	1.3	1.2	4.8
07134+1005	1988 Apr 09		2.21	1.96	1.66	0.67	−0.11	−2.05

NOTE.—Observational uncertainties (in mag) are as follows—visible: 0.01 at CTIO, 0.04 at Yerkes; infrared: <0.03 at KPNO and SAAO, <0.02 (*J* through *M*) and <0.05 (8.75 through 19.5 μm) at UKIRT.

[a] Observational uncertainty of ±0.16.

[b] Observational date was 1988 Apr 8.

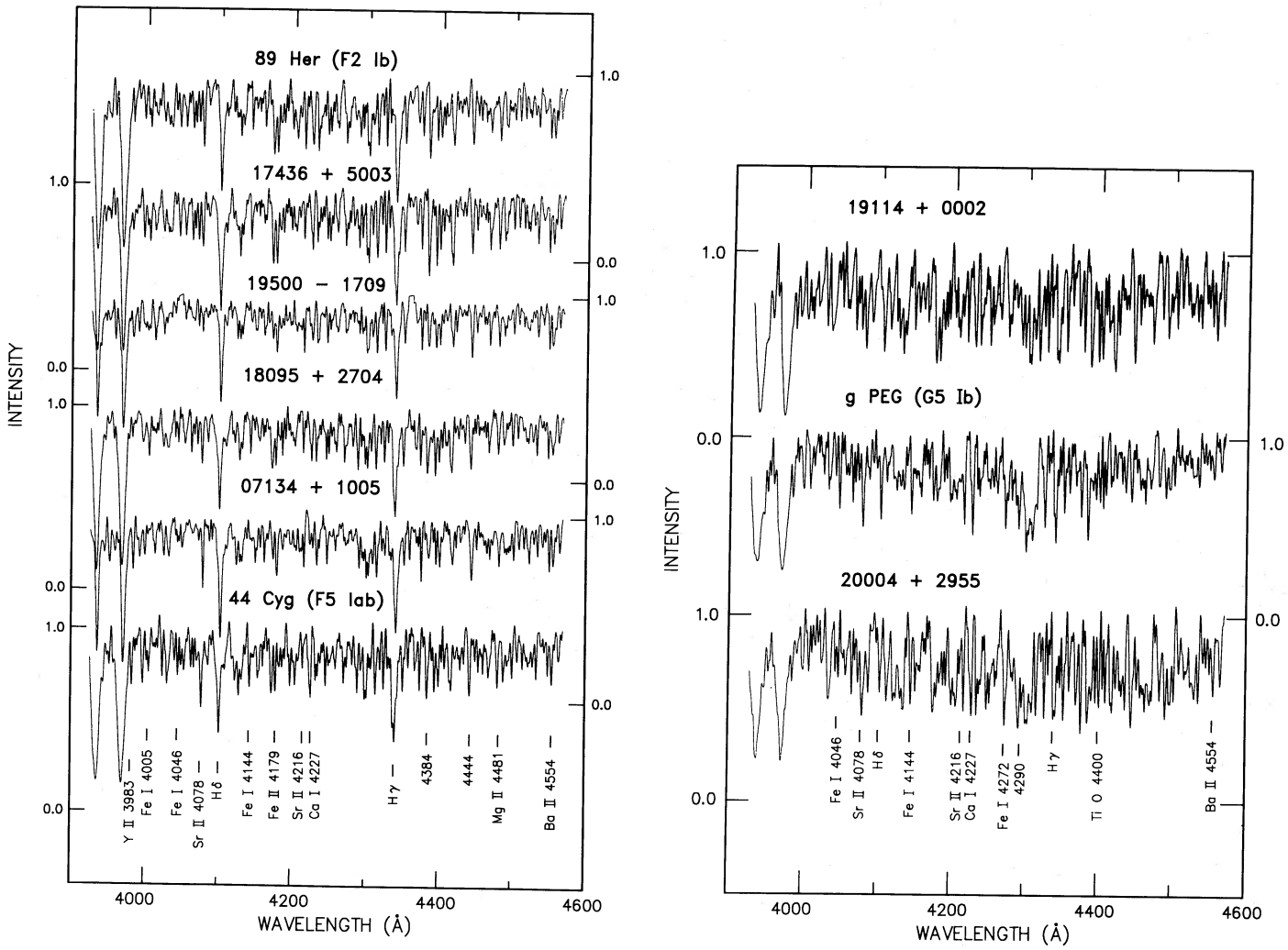

FIG. 1.—Optical spectra of five of these sources and IRAS 18095+2704, together with several classification standards. (*a*) The F supergiants. (Note that in the spectrum of 19500−1709, two mercury night-sky emission lines have been truncated slightly above the continuum level.) (*b*) The G supergiants.

These will be published as part of a separate study of the variability of these objects. IRAS 19114+0002 stands out as a high-velocity object, with a radial velocity of +88 km s^{-1}.

b) Discussion of Individual Objects

IRAS 07134+1005.—The published spectral type of the object is F5 I (Nassau, Stephenson, and MacConnell 1965). The object has been observed in the Walraven intermediate-band *VBLUM* system by Pel (1976) and by van Genderen, van Driel, and Greidanus (1986), with the later investigators commenting on the reddness of its colors. The *B* and *V* magnitudes listed in Table 4 are those transformed by van Genderen, van Driel, and Greidanus (1986) to the Johnson system. With $(B-V) = 0.90$, the object is clearly reddened. CO emission has been detected from this object (Zuckerman, Dyck, and Claussen 1986) and at a relatively high velocity. Zuckerman and Dyck (1986) classify this object as oxygen-rich on the basis of its *IRAS* colors.

This object is not included in the *IRAS* LRSC. A spectrum was extracted from the LRS data base. The spectrum is almost flat between 10 and 18 μm and has a strong emission feature at 21 μm. This feature is too wide to be due to spectral line emission and does not appear to be due to silicates, for there is no corresponding feature at 10 μm.

One might suspect that this odd spectrum is due to causes other than the source itself. For example there could be another source near IRAS 07134+1005 which is entering the focal plane just after IRAS 07134+1005 and thus producing the rise near 21 μm. That possibility was checked by looking for nearby *IRAS* point sources, and none was found anywhere near IRAS 07134+1005 that was bright enough at 12 μm to produce contamination of the spectrum. Also the individual scans all show the same features. Thus it is not obvious that there is any contamination or instrumental problems affecting the spectrum. There are a few other sources with similar LRS spectra. One of these is IRAS 22272+5435 which is associated with the K5 I star SAO 34504. The source appears to have the 21 μm emission feature but it is relatively weak. It also displays a drop in its spectrum near 11 μm similar to that of IRAS 07134+1005. This source is discussed by Pottasch and Parthasarathy (1988), who attribute the features to silicate absorption.

IRAS 10215−5916.—The object was identified with CoD −58°3221 by Bidelman (1986), who also listed a spectral type of G5: I by Sanduleak. It lies 55″ north of the position of

RAFGL 4106, and we assume them to be the same source, as the *IRAS* 25 μm flux is similar to the 27.4 μm flux of RAFGL 4106 (Price and Murdock 1983) and there is no other *IRAS* source closer to this bright RAFGL source. The object is extremely red, with $(B-V) = 1.50$. At its low galactic latitude, $b = -2°$, much of this might be interstellar.

IRAS 12175−5338.—This star has an earlier spectral type than any of the others in our study, A9 Iab (Stephenson and Sanduleak 1971). It is somewhat reddened. It is not in the LRSC and the spectrum extracted from the LRS data base is extremely noisy and not very useful for detailed study, as the 12 μm flux density is too low for a reasonable quality LRS spectrum to be observed. However, it does show an increase in flux from 10 to 20 μm, in agreement with the broad-band *IRAS* measurements.

IRAS 17436+5003.—This object is well studied, and its visible and infrared flux distribution have been analyzed and discussed previously by Parthasarathy and Pottasch (1986). The spectrum of the system has been carefully classified as F3 Ib (Fernie and Garrison 1984), and we adopt it as a secondary standard for our classifications. Older abundance analyses yield differing results as to whether the object is metal poor or not. A recent study by Bond and Luck (1987) concludes that it is slightly metal poor, and Fernie and Garrison (1984) conclude that is is only slightly metal poor, if at all.

Our new *UBV* photometry leads to magnitudes similar to those of Fernie (1983) and Percy and Welch (1981), with our observations indicating that the object was somewhat brighter and bluer than average when we observed it. The mean *UBVRI* values of Fernie (1983) are used to form the flux distribution and these are listed in the summary in Table 4. Little reddening is indicated for the system. A polarization study shows that the object has a small but significant intrinsic polarization, 0.6%, with no wavelength dependence, which is interpreted as evidence for large (>0.3 μm) dust grains uniformly distributed around the source (Joshi *et al.* 1987). Near-infrared *JHKL* photometry has been published by Humphreys and Ney (1974), and AFGL 20 and 27 μm photometry has been published by Price and Murdock (1983). The *IRAS* spectrum was extracted from the LRS data base and is noisy below 12 μm where the flux density is low. The object is a known quasi-periodic light and velocity variable, with a range in V of 0.08 mag (Fernie 1983; Burki, Mayor, and Rufener 1980).

IRAS 19114+0002.—The spectrum of the object has been previously classified as G5: Ia (Buscombe 1984), G4 0–Ia (Keenan 1983), and G Ia (Bidelman 1981). The observed color index, $(B-V) = 1.60$, is very red for mid-G spectral type. At its low latitude, $b = -5°$, much of this might be interstellar. The source is associated with RAFGL 2343, and infrared magnitudes are given by Ney and Merrill (1980) and Price and Murdock (1983). There is no LRSC classification, and a weak 10 μm feature is detectable on the extracted spectrum. Zuckerman and Dyck (1986) consider it to be oxygen-rich on the basis of its *IRAS* colors.

CO emission has been measured from the object, at a large velocity relative to the LSR (Zuckerman and Dyck 1986; Likkel *et al.* 1987). The expansion velocity (V_e) of 33 km s^{-1} is higher than the typical expansion velocity of the circumstellar envelopes of AGB stars. Such a high expansion velocity is more typical of supergiants (Jones 1987).

IRAS 19244+1115.—This source is associated with the well-known infrared object IRC +10420, one of the strongest sources in the sky at 10 and 20 μm. It is known to vary irregularly in light and has been assigned the variable star name V1302 Aql. The photographic magnitude increased by about 1.4 mag from 1920 through 1975, while from 1900 through 1920 the light level was near the middle of this range (Gottlieb and Liller 1978). *UBVRI* and 2.2 to 22 μm photometry has been published by Humphreys *et al.* (1973), who noted the similarity of the infrared flux distribution with that of η Car. *UBV* observations made 2 yr after those listed by Humphreys *et al.* showed a similar light level (Craine and Tapia 1975), as did the infrared observations of Thomas, Robinson, and Hyland (1976).

The spectrum has been classified as F8–G0 I (Humphreys *et al.* 1973) and F8 Ia (Giguere, Woolf, and Webber 1976). High-resolution infrared spectra reveal CO band lines at 4.6 μm with P Cygni profiles (Fix and Cobb 1987), and both the stellar and outflow velocities are in agreement with the 18 cm OH velocities. The photospheric absorption lines indicate a radial velocity 30 km s^{-1} larger than the OH velocity, which Fix (1981) attributes to scattering of photons from the expanding shell (Kwok 1976). New emission lines have recently been observed in the near-infrared spectrum (Irvine 1986).

IRC +10420 is a strong source of OH emission and has been studied by several investigators. It shows a variability in total flux over several months, and a number of highly circularly polarized individual features in its blueshifted and redshifted peaks (Mutel *et al.* 1979). OH and SiO emission have both been measured, with similarly large radial velocities and with similar expansion velocities (Bowers, Johnston, and Spencer 1983; Olofsson *et al.* 1982). A mass-loss rate of $2 \times 10^{-4}\ M_\odot$ yr^{-1} was calculated by Bowers, Johnston, and Spencer (1983), based upon a distance of 3.4 kpc (Mutel *et al.* 1979), which is probably overestimated. CO and HCN have both been observed (Bachiller *et al.* 1988; Jewell, Snyder, and Schenewerk 1986, respectively), and SO_2 has been detected by Guilloteau *et al.* (1986).

A VLA study of OH emission by Bowers (1984) indicates a clumpy, asymmetric distribution of emission, which he fits with an expanding spherical shell model. In contrast, Diamond, Norris, and Booth (1983) interpret their MERLIN study of OH as indicating a bipolar nebula. Recently, Ridgway *et al.* (1986) have used infrared speckel interferometry to study the dust shell of IRC +10420. They find no convincing evidence of asymmetry in their data, and model their data to determine an optical depth of 0.7 ± 0.3 at 3.4 μm and an inner dust shell radius of $0''.125 \pm 0''.015$. We will later compare their results with our derived values.

IRAS 19500−1709.—The spectral type assigned to this object is cF3 by Houk (Bidelman 1986) and F2–3 by Parthasarathy, Pottasch, and Wamseker (1988). Our *UBV* observations indicate little reddening.

IRAS 20004+2955.—This source is associated with the irregular variable V1027 Cyg, which has an observed range of variability of 1 mag in the photographic (Wachmann 1961). The spectrum has been classified as G7 Ia (Keenan and Pitts 1980) and K0 Ia (Roman 1973). The observed color index, $(B-V) = 2.34$, is very red. At its low latitude, $b = 0°$, much of this might be interstellar. The LRS classification of 69, which means a 10 μm silicate emission feature on a red continuum, is similar to that of 18095+2704. An observation at 1612 MHz did not detect OH emission (Eder, Lewis, and Terzian 1987).

c) *Observational Summary*

In Table 4 are collected the visible-band and near-infrared data available for the program objects. Where multiple obser-

TABLE 4

SUMMARY OF GROUND-BASED OBSERVATIONS

IRAS ID	*U*	*B*	*V*	*R*	*I*	*J*	*H*	*K*	*L*	*M*	*N*	*Q*	[27]	Spectral Types	A_v
07134+1005	...	9.13	8.23	...	...	6.92	6.66	6.65	6.43	6.10	...	...	...	F5 I	0.6
10215−5916	11.22	10.24	8.73	7.20	5.78	4.61	3.49	3.02	2.58	...	...	−5.8	−6.8	G5: I	2
12175−5338	10.15	9.68	9.30	8.92	8.63	8.43	8.24	8.14	8.03	...	...	...	...	A9 Iab	0.5
17436+5003	7.82	7.54	7.08	6.67	6.42	5.83	5.98	6.02	5.83	...	...	−2.5	−3.1	F3 Ib	0.1
19114+0002	10.81	9.49	7.89	...	...	5.00	4.52	4.28	4.05	3.71	0.1	−4.1	−5.0	G5 Ia	2
19244+1115	15.7	13.9	11.2	8.7	7.0	4.9	3.7	2.7	0.6	−0.65	−4.6	−6.4	−6.7	F8 Ia	3
19500−1709	9.34	9.19	8.67	...	...	7.18	6.92	6.8	6.57	6.14	...	...	...	cF3	0.4
20004+2955	13.3	11.28	8.94	...	...	4.79	4.15	4.01	3.38	3.06	...	...	...	G7 Ia	2.5–3

vations are available, average values are listed. The *R* and *I* observations are on the Johnson system, with the Cousins system values transformed using the relationships given by Bessell (1979) and Celis (1986). The ground-based data are combined with the *IRAS* data, and the flux distribution plotted for each object in Figures 2–9. In cases where the two halves of the LRS do not coincide in the overlapping wavelengths, one-half was shifted to match the other and the entire LRS scaled with respect to the 12 μm photometry point after it was first convolved with the 12 μm band instrumental profile.

For IRAS 20004+2955, which varies by 1 mag in the visible, the lack of simultaneity of the observations will affect the detailed flux distribution, although the general shape of the spectrum will be represented. IRAS 19244+1115 has displayed significant historical variability, although there is no documentation of present variability at greater than the 10% level. None of the other objects is known to vary by as much as 10%, and the combination of data should accurately represent the spectrum. Flux calibrations for *UBVRI* are taken from Hayes (1979), and near-infrared from calibration coefficients provided by Joyce. Conversion factors to flux measurements for the Walraven system were taken from Lub *et al.* (1979). Values have been estimated for the reddening and visual extinction of each object, assuming a distance of a few kiloparsecs. These have been derived from the studies of Neckel and Klare (1980) and Burstein and Heiles (1982) for objects in and out of the Galactic plane, respectively. These estimated values of extinction are listed in the rightmost column of Table 4, and they are in good agreement with the general comments regarding the observed reddening of the individual objects.

CO emission has been observed for four of these sources and expansion velocities measured. Except for 19244+1115, none of the sources has had additional molecular lines detected. The molecular line observations have been summarized in Table 5.

IV. MODELS AND RESULTS

The prominence of the photospheric emission in all of the objects suggests the following two possibilities: (1) the circumstellar dust is in the form of a disk or torus which we are viewing nearly face-on; or (2) the circumstellar dust is distributed spherically and the envelope is optically thin in all wavelengths longward of 0.5 μm. In the absence of evidence for asymmetry, we shall adopt the second assumption as it is the simpler of the two. The optically thin approximation is particularly attractive considering the evolutionary nature of these objects. If they are indeed post-AGB objects, the mass-loss process would have been terminated sometime in the past, probably when the star was at the tip of the AGB (defined as $t = 0$). As the star evolves to the left of the H-R diagram, the remnant dust envelope will continue to expand into the interstellar medium, leaving a "hole" between the inner base of the envelope and the surface of the star. If the dust mass-loss rate ($\dot{M}_d$) has been constant in the preceding several thousand years, the density distribution of the envelope would have a form of $r^{-\alpha}$ with $\alpha = 2$, and the optical depth of the envelope will decrease linearly with time ($\tau \propto r^{-1} \propto t^{-1}$). A mass-loss

TABLE 5

SUMMARY OF MOLECULAR LINE OBSERVATIONS

IRAS ID	Line	V_{LSR} (km s^{-1})	V_e (km s^{-1})	Reference	Remarks
07134+1005	CO	+71.0	10.0	a	ND in H_2O[b]
10215−5916	...	...	...	...	...
12175−5338	...	...	...	...	...
17436+5003	CO	−36	11.5	c	ND in H_2O[b]
19114+0002	CO	+99	33	c	ND in H_2O[b]
	CO	+105.0	33.9	d	ND in HCN[e]
19244+1115	OH	+73.7	33.0	f	ND in H_2O[g]
	SiO	+79	35	h	...
	HCN	+78	39	i	...
	CO	+73	47	j	...
19500−1709	CO	+25	11	c	...
20004+2955	...	...	...	...	ND in OH[k]

REFERENCES.—(a) Zuckerman, Dyck, and Claussen 1986; (b) Zuckerman and Lo 1987; (c) Likkel *et al.* 1987; (d) Zuckerman and Dyck 1986; (e) Lucas, Guilloteau, and Omont 1988; (f) Bowers, Johnston, and Spencer 1983; (g) Nyman, Johansson, and Booth 1986; (h) Olofsson *et al.* 1982; (i) Jewell, Snyder, and Schenewerk 1986; (j) Bachiller *et al.* 1988; (k) Eder, Lewis, and Terzian 1987.

NOTE.—ND stands for no detection in the particular molecular line indicated.

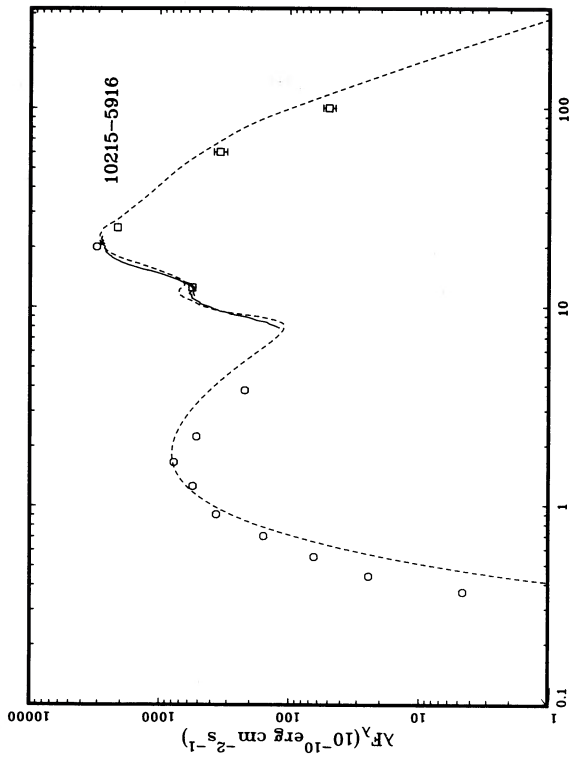

FIG. 3

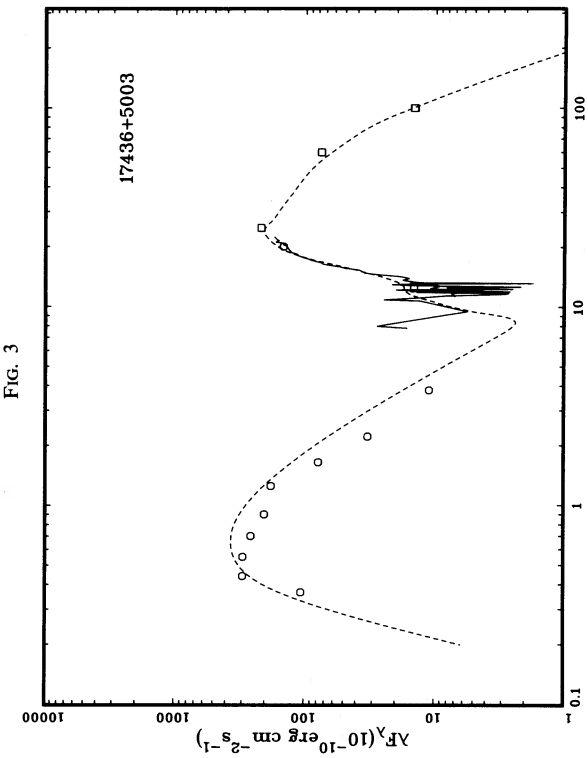

FIG. 5

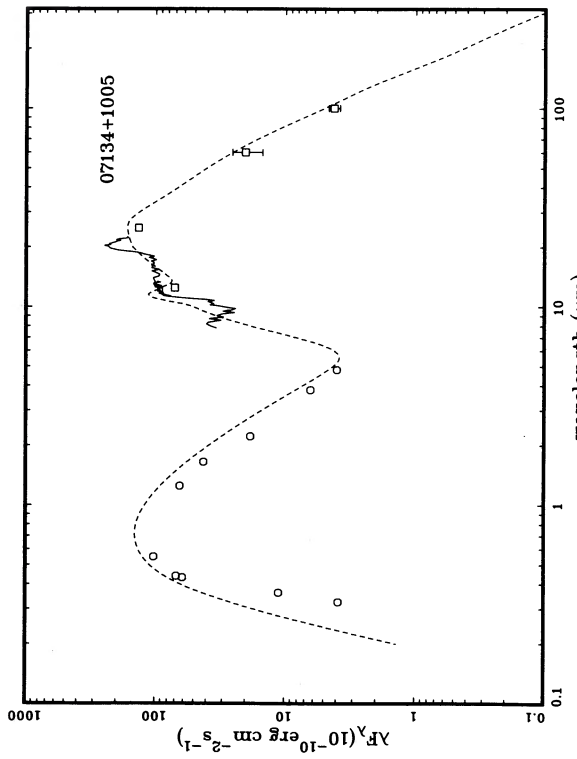

FIG. 2

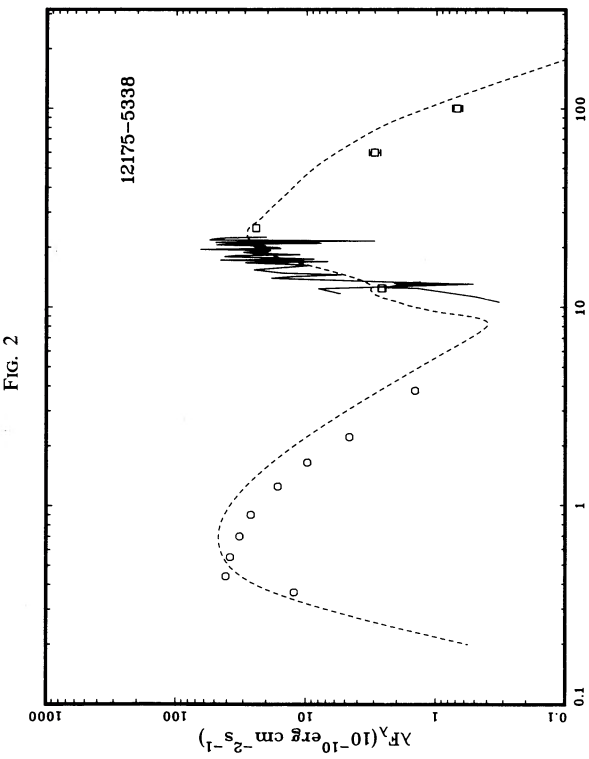

FIG. 4

FIG. 2.—Combined optical and infrared spectrum of 07134+1005. The circles and squares are ground-based and *IRAS* measurements, respectively, for Figs. 2–9. The data between 7 and 22 μm are from the *IRAS* LRS data bank and have been normalized to the 12 μm point after convolution with the 12 μm instrumental profile for Figs. 2–9. The dashed line represents the model fit to the entire energy distribution. Details of the fit are described in the text.

FIG. 3.—Spectrum of 10215−5916

FIG. 4.—Spectrum of 12175−5338

FIG. 5.—Spectrum of 17436+5003

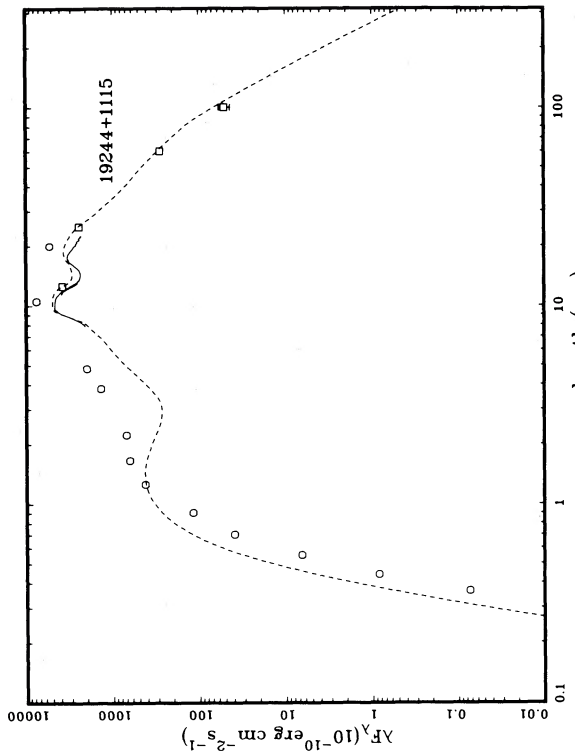

FIG. 7.—Spectrum of 19244 + 1115

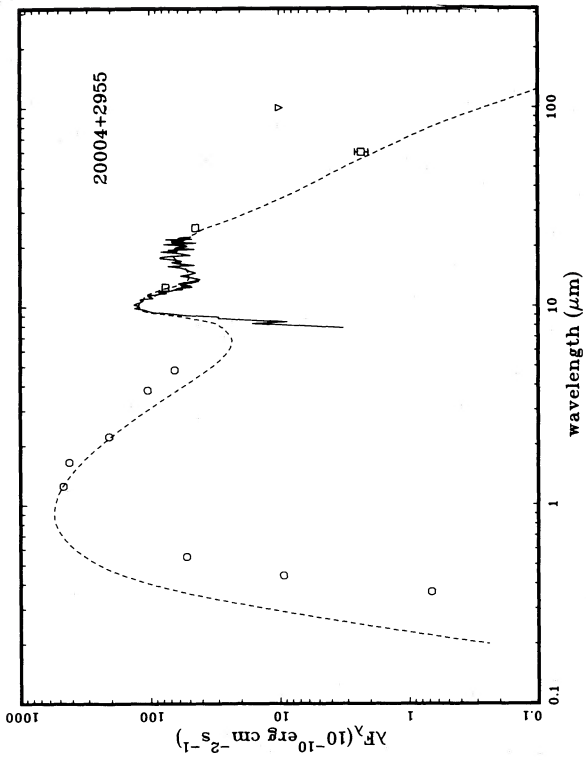

FIG. 9.—Spectrum of 20004 + 2955. The inverted triangle at 100 μm represents an upper limit.

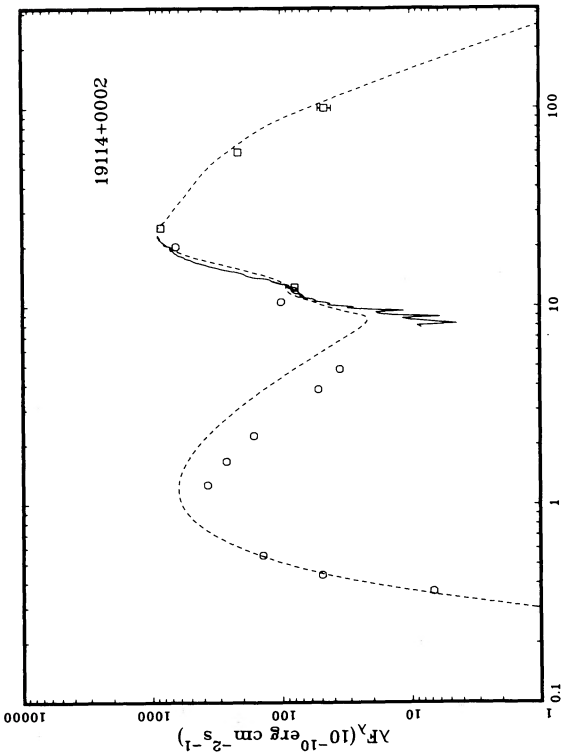

FIG. 6.–Spectrum of 19114 + 0002

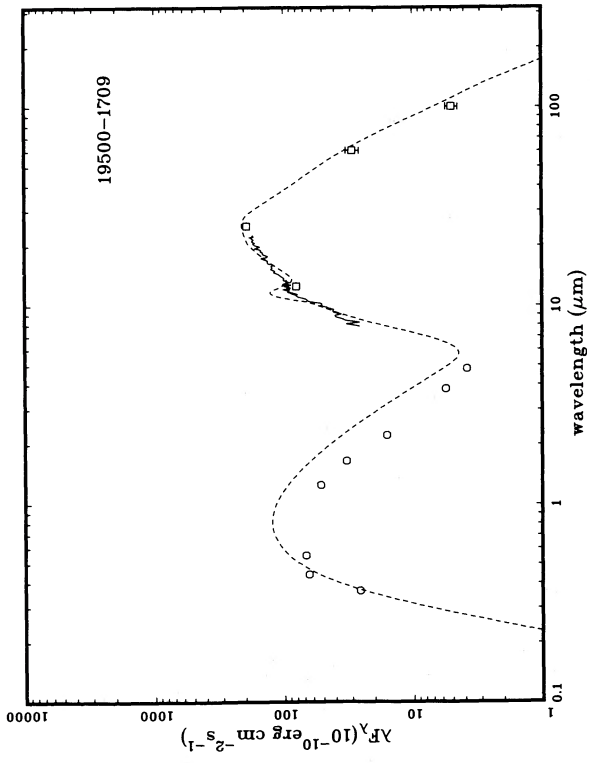

FIG. 8.—Spectrum of 19500 − 1709

rate which increases with time on the AGB would be represented by $\alpha > 2$. While the progenitors of these stars might have had optically thick envelopes during the AGB and might have appeared as infrared objects with no bright optical counterparts, the circumstellar envelopes are likely to have become optically thin after several hundred years of post-AGB evolution.

While the dust envelope is likely to be optically thin, the observed energy distributions of the objects indicate that comparable amounts of energy are emitted in the visible and the infrared. This combination of a large fraction of the stellar luminosity in the form of reemitted infrared light and at the same time a bright central star puts severe constraints on a model. Model fits to the energy distributions of these eight stars have been obtained using a radiative transfer calculation. Details of the calculations are given in Volk and Kwok (1989).

The model fittings to the flux distribution from 0.4 to 100 μm are shown in Figures 2 through 9. Three quantities—L_*/D^2, r_{in}/D, and $(\dot{M}/V)/D$—are derived from the model fittings, where L_* is the stellar luminosity, D is the distance, r_{in} is the inner radius of the dust envelope, V is the dust expansion velocity, and $\dot{M}$ is the total (gas plus dust) mass-loss rate. The silicate grain opacity function of Volk and Kwok (1988) is used and the gas-to-dust mass ratio is assumed to be 160. For two sources with no obvious silicate features (07134+1115 and 19500−1709), the grain opacity function for SiC is used instead.

The stellar temperature (T_*) is estimated from the spectral types of the stars and is derived from Allen (1973). The temperature of 12175−5338, with a spectral classification of A9 Iab, is the average of values taken from Johnson (1966) and Flower (1977). We find that errors in T_* of a few hundred degrees do not have a major effect on the overall energy distribution.

In almost every case, the observed color temperature of the photospheric component is significantly redder than the stellar temperature expected from the spectral type. As in the case of IRAS 18095+2704, we find that another component of extinction is required in addition to the circumstellar reddening inherent in the model. In the present model fits, we assume an additional source of extinction (presumably interstellar) which has a λ^{-1} dependence on opacity. The additional extinction (A_v) varies greatly among the objects. It is in almost every case, however, consistent with the estimated interstellar extinction listed in Table 4. The notable exception is 10215−5916, where there is evidence for a large additional circumstellar component, possibly a more extended dust shell farther from the star. The object may be associated with the Carina complex, which could explain the large extinction. A summary of the parameters used to produce the model fits in Figures 2 through 9 is given in Table 6. Note that the model was adjusted to give the best fits in the infrared region and provide a reasonably good representation of the visible and near-infrared flux. The fit to the visible and the near-infrared could perhaps be improved in some cases by further slight adjustments of the model and dust parameters. The fit of the model to the observed flux distribution of each object is discussed below.

IRAS 07134+1005.—The model of this source fits the photometry very well over the entire wavelength range. The colors of this source suggests that it left the AGB only a short time ago. The LRS of this source is very peculiar with a strong emission feature at 21 μm. In the absence of a better knowledge of the grain material and the fact that this source is carbon-rich (Kwok and Hrivnak 1989), the SiC opacity function is used in the fitting. A relatively small amount of extinction is required to produce agreement with the short-wavelength data. The final model has an $\tau(11.3\ \mu m)$ of 5.0 at $t = 0$, $\alpha = 2$, and a present inner radius (r_{in}) of 50 times r_{in} at $t = 0$. Note that the inner radius at $t = 0$ is the dust condensation radius. If the distance is 1 kpc or less, the luminosity and mass-loss rate for this source are relatively low.

IRAS 10215−5916.—The *IRAS* data are well fitted by a model with an initial 9.7 μm optical depth of 20.0, $\alpha = 2.5$, and an inner radius 100 times the initial value. Slightly lower initial optical depths are also possible. The final model has an optical depth of 0.04 at 9.7 μm. Despite the low optical depth the model 10 μm feature is slightly stronger than observed. There is some discrepancy between the near-infrared observations and the model fit, with the observations falling below the model. The amount of extinction that is needed to fit the shorter wavelength points is rather large—$\sim$6 mag at V. This source is in the direction of the Carina complex and may be associated with it. This would suggest a distance of $\approx$2 kpc. The source is quite bright at 25 and 60 μm leading to a very high estimated luminosity, a bolometric magnitude of about $\sim$7.5 for a distance of 1 kpc and $\sim$9.0 for a distance of 2.0 kpc.

IRAS 12175−5338.—This object has unusually low 25/60 and 60/100 colors, so low that even models with $\alpha = 3.0$ were unable to properly match the colors. The LRS spectrum of 12175−5338 is very noisy and steeply falling, but baseline difficulties in the extraction make it difficult to be sure of the continuum slope. The spectrum does not show any obvious feature. The best-fit model has an optical depth of 0.018 at 9.7 μm, from an initial optical depth of 60.0. A still higher initial optical depth might work slightly better in the infrared but would cause problems at shorter wavelengths. A lower optical

TABLE 6

MODEL FITTING PARAMETERS

IRAS ID	α	r_{in}/D (10^{15} cm/kpc)	$\dot{M}/V/D$ ($M_\odot$ yr^{-1}/km s^{-1}/kpc)	L_*/D^2 ($L_\odot$/kpc^2)	T_* (K)	A_v (mag)
07134+1005	2	3.2	3.1(−7)	1725	6600	0.7
10215−5916	2.5	47.8	1.4(−5)	80000	5000	7.1
12175−5338	3	13.5	1.0(−5)	800	7400	1.4
17436+5003	2.5	28.2	1.2(−5)	3654	7000	0.7
19114+0002	2.5	41.5	2.4(−5)	15873	5000	3.0
19244+1115	2	2.5	1.8(−6)	24000	6000	2.4
19500−1709	2	4.0	3.6(−7)	2335	7000	1.4
20004+2955	3	3.2	5.0(−7)	6042	5000	3.6

depth model track cannot reach the proper 12/25 color for this α value. The adopted model results in a very low estimated luminosity for the star.

IRAS 17436+5003.—Based on the *IRAS* colors, this object is probably the most evolved among the eight. An inner shell radius of about 180 times the initial value gives a good fit to the colors for an initial 9.7 μm optical depth of 50.0 and $\alpha = 2.5$. As with several of the other objects, the model has too strong a feature at 10 μm. In this case the 10 μm feature has an optical depth of 0.04. A relatively small amount of extinction produces reasonable agreement at short wavelengths.

IRAS 19114+0002.—This source has a spectral type later than that of IRAS 17436+5003 but the infrared properties seem very similar. The best-fit values for IRAS 19114+0002 are much the same as those for IRAS 17436+5003—an initial optical depth of 50.0, $\alpha = 2.5$, and an inner shell radius of 140 times the initial value. In this case the amount of extinction required for short-wavelength agreement is 4 times larger than for 17436+5003. Here the LRS data do not show the beginning of the stellar continuum, which should in principle be seen just at the blue edge of the spectrum. As this source is several times brighter than 17436+5003, the derived luminosity is larger and the time since the end of the AGB is probably on the order 1000 yr. However, 17436+5003 could easily be twice as far away as 19114+0002, in which case, according to the models, these two sources were virtually identical when on the AGB.

IRAS 19244+1115.—IRC +10420 is clearly a case where the end of the mass loss, whether permanently or not, occurred very recently. Here the near-infrared data imply that the mass loss did not end instantly as these models assume. This makes the fitting difficult. The development of the strong 10 μm emission feature so early in the evolution implies that the initial optical depth was not extremely high. The best fit that was found was for an initial optical depth of 7.5, $\alpha = 2.0$, and an inner radius 10 times the initial value. A moderate amount of extinction is needed to make the model match the shorter wavelength points. The derived shell inner radius of 0.0008 pc is consistent with the observations of Ridgway *et al.* (1986) using speckle interferometry if the distance to the source is between 1.2 and 1.5 kpc. However, it is not clear that their angular diameter corresponds to our inner shell radius since they were working at 3.4 μm, and backfilling of the cavity would complicate matters at this wavelength. For comparison, our model inner radius for the dust shell is 0".17 and the observed near-infrared inner radius is 0".125 $\pm$ 0".015. They derive an optical depth of 0.7 $\pm$ 0.3 at 3.4 μm and a maximum temperature of 750 K $\pm$ 50 K for the dust. The optical depth in our model is 0.19 at 3.4 μm while the inner shell temperature is about 475 K. In view of the limitations of the model in this instance this agreement is satisfactory.

IRAS 19500−1709.—The LRS spectrum of this source is slightly unusual in that the blue part of the spectrum declines in a way that probably precludes there being any 10 μm feature. Again the SiC opacity function is used in view of the lack of a better alternative. The best color fit was obtained for an initial optical depth of about 5.0 at 11.3 μm, $\alpha = 2.0$, and an inner radius equal to 55 times the initial value. From the redness of its colors, it appears just slightly more evolved than 07134+1005. While the observed spectrum cannot be reproduced in detail by the SiC model, the color match is excellent on the 12/25/60 color-color diagram. It should be noted that a slightly better fit in the near-infrared is obtained if the initial optical depth is 10 rather than 5. However, such a model does not fit the *IRAS* colors quite as well. If the correct dust opacity function were available, the LRS spectrum would allow some discrimination between the two cases. A moderate amount of extinction is needed to match the short-wavelength data. For the optical depth 10.0 model this amount would be much smaller.

IRAS 20004+2955.—With a strong 10 μm emission feature and an unusually small 25/60 color, this source was rather difficult to model. With $\alpha = 3.0$, a reasonable result was found for an initial optical depth near 2.0 and an inner radius of 25 times the initial value, giving a model optical depth of 0.015 at 9.7 μm. The short-wavelength data are difficult to match, as the near-infrared data and the optical data are not satisfied by the same amount of extinction. This may indicate that the stellar effective temperature is lower than the 5000 K value which was used in the models. The near-infrared data can be matched by a value of $A_v = 1.2$, while to match the optical data, a value 3 times this amount is required. At least some of this difficulty may be attributed to the known large variability of the source.

V. DISCUSSION

We regard as strong evidence of the PPN nature of these objects the low dust temperatures and correspondingly large derived inner radii of the dust shells relative to the dust condensation radii. It appears that mass loss has clearly ceased and that the circumstellar envelopes have continued to expand. The dust temperatures found for these objects (150–300 K) are intermediate between those of the late-asymptotic giant branch stars (300 K; Kwok, Hrivnak, and Boreiko 1987) and planetary nebulae (40–150 K; Pottasch *et al.* 1984). They are, in fact, similar to those of compact planetary nebulae (150–250 K; Kwok, Hrivnak, and Milone 1986). The spectral types of the central stars, the absence of large-amplitude photometric variability, and the presence of CO envelopes are all consistent with this PPN interpretation. The detached envelope model discussed in the last section is able to fit the observations as a whole reasonably well.

Based upon the parameters derived from these models, one can derive the time t since the termination of mass loss as a function of distance. Five of the eight objects have measured gas expansion velocities from molecular line (CO or OH) observations. If the dust and gas drift velocity is small (Kwok 1975), t can be calculated by assuming that the dust velocity can be approximated by the gas expansion velocity V_e. Thus $t = r_{in}/V_e$ and the time scales with the distance. If one assumes that the sources are each at a distance of 1 kpc, the derived times and thus the ages since the termination of the AGB phase are 100, 120, 400, and 800 yr for 07134+1005, 19500−1709, 19114+0002, and 17436+5003, respectively. While we are not suggesting that each of these objects is at the same distance of 1 kpc, the calculated values do emphasize the short time scales involved since the end of active mass loss and the detachment of the circumstellar shell.

Pottasch and Parthasarathy (1988) derive distances for their sample of F and G-type infrared stars by the method of spectroscopic parallax. However, if these stars are not supergiants but intermediate-mass stars in post-AGB evolution, then such a method is not appropriate as the true luminosities are not known. For example, Pottasch and Parathasarathy (1988) assume a visual absolute magnitude of −8.0 for IRAS 19114+0002, which is above the AGB limit of $M_{bol} \approx -7$ (cf. Iben and Renzini 1983). Decreasing their distances would also

give more reasonable values for the total dust mass in the envelopes.

Another interesting aspect of the present model is the predicted increase in visible brightness of the objects as the dust envelope expands and the optical thickness declines. Systematic brightening should be detectable by photometric monitoring over several decades.

In this paper, we explain the infrared excess by dust emission from a spherical circumstellar envelope. The nearly equal amount of emission from the star and the envelope greatly restricts the allowable parameter space. As suggested in § IV, an alternative is a disk or toroidal model. Since the (optically thin) infrared emission is not affected by the geometry, the varying degree of brightness of the photospheric component and the value of A_v adopted for the model in excess of the expected interstellar contribution can be the result of the varying inclination angle of the disk with respect to line of sight to the observer. We intend to further pursue this possibility with a two-dimensional continuum radiative transfer code.

VI. SUMMARY AND CONCLUSIONS

From low-color temperature objects in the *IRAS* catalog, we have identified a number of candidates for proto–planetary nebulae. Ground-based optical and infrared observations reveal that these objects have bright optical counterparts, which are generally of spectral types F and G and which display spectral characteristics of supergiants. The most interesting aspect of the energy distribution of these objects is that a significant amount of energy is emitted in the far-infrared, sometimes more than that observed in the visible. These observational results are interpreted by means of a proto–planetary nebulae model which assumes that the far-infrared component originates from the remnant of the circumstellar envelope ejected by the star's AGB progenitor. The expansion of this envelope and the rapid evolution of the central star toward the blue side of the H-R diagram have led to the reemergence of the light of the central star from the envelope. The spectral types of the optical counterparts of these infrared objects are consistent with such an explanation. The observed energy distribution from 0.4–100 μm is fitted by a dust radiative transfer model, and the model results suggest that these objects left the AGB several hundred years ago.

We thank D. Geisler, R. Joyce, and P. Whitelock, who have kindly obtained observations for us at Cerro Tololo Inter-American Observatory, Kitt Peak National Observatory, and South African Astronomical Observatory, respectively. We also acknowledge the service provided by T. Geballe and others of the United Kingdom Infrared Telescope staff in obtaining infrared observations, and the allocation of observing time at Yerkes Observatory. This research was supported by grants to B. J. H. from NASA administered by the American Astronomical Society and to S. K. from the Natural Sciences and Engineering Research Council of Canada, and under NASA's *IRAS* Astrophysical Data Program and funded through the Jet Propulsion Laboratory. B. J. H. and K. M. V. acknowledge, respectively, the support of Valparaiso University through a University Research Professorship, and a Natural Sciences and Engineering Research Council of Canada Postdoctoral Fellowship.

REFERENCES

Allen, C. W. 1973, *Astrophysical Quantities* (London: Athlone).
Atlas of Low Resolution *IRAS* Spectra. 1986, *IRAS* Science Team, prepared by F. M. Olnon and E. Raimond (*Astr. Ap. Suppl.*, **65**, 607).
Bachiller, R., Gomez-Gonzalez, J., Bujarrabal, V., and Martin-Pintado, J. 1988, *Astr. Ap.*, **196**, L5.
Bessell, M. S. 1979, *Pub. A.S.P.*, **91**, 589.
Bidelman, W. P. 1981, *A.J.*, **86**, 553.
———. 1986, private communication.
Bond, H. E., Carney, B. W., and Grauer, A. D. 1984, *Pub. A.S.P.*, **96**, 176.
Bond, H. E., and Luck, R. E. 1987, in *IAU Colloquium 95, The Second Conference on Faint Blue Stars*, ed. A. G. D. Philips, D. S. Hayes, and J. W. Liebert (Schenectady: L. Davis), p. 527.
Bowers, P. F. 1984, *Ap. J.*, **279**, 350.
Bowers, P. F., Johnston, K. J., and Spencer, J. H. 1983, *Ap. J.*, **274**, 733.
Burki, G., Mayor, M., and Rufener, F. 1980, *Astr. Ap. Suppl.*, **42**, 383.
Burnstein, D., and Heiles, C. 1982, *A.J.*, **87**, 1165.
Buscombe, W. 1984, *MK Spectral Classifications, Sixth General Catalog* (Evanston: Northwestern University).
Celis, S. L. 1986, *Ap. J. Suppl.*, **60**, 879.
Crane, E. R., and Tapia, S. 1975, *Pub. A.S.P.*, **87**, 131.
Diamond, P. J., Norris, R. P., and Booth, R. S. 1983, *Astr. Ap.*, **124**, L4.
Eder, J., Lewis, B. M., and Terzian, Y. 1987, *Ap. J. Suppl.*, **66**, 183.
Fernie, J. D. 1983, *Ap. J.*, **265**, 999.
Fernie, J. D., and Garrison, R. F. 1984, *Ap. J.*, **285**, 698.
Fix, J. D. 1981, *Ap. J.*, **248**, 542.
Fix, J. D., and Cobb, M. L. 1987, *Ap. J.*, **312**, 290.
Flower, P. J. 1977, *Astr. Ap.*, **54**, 31.
Gehrz, R. D. 1972, *Ap. J.*, **178**, 715.
Giguere, P. T., Woolf, N. J., and Webber, J. C. 1976, *Ap. J. (Letters)*, **207**, L195.
Gottlieb, E. W., and Liller, W. 1978, *Ap. J.*, **225**, 488.
Guilloteau, S., Lucas, R., Nguyen-Q-Rieu, and Omont, A. 1986, *Astr. Ap.*, **165**, L1.
Hayes, D. S. 1979, *Dudley Obs. Rept.*, **14**, 297.
Hrivnak, B. J., Kwok, S., and Volk, K. M. 1988, *Ap. J.*, **331**, 832.
Humphreys, R. M., and Ney, E. P. 1974, *Ap. J.*, **190**, 339.
Humphreys, R. M., Strecker, D. W., Murdoch, T. L., and Low, F. J. 1973, *Ap. J. (Letters)*, **179**, L49.
Iben, I., Jr., and Renzini, A. 1983, *Ann. Rev. Astr. Ap.*, **21**, 271.
Irvine, C. E. 1986, *IAU Circ.*, No. 4286.
Jewell, P. R., Snyder, L. E., and Schenewerk, M. S. 1986, *Nature*, **323**, 311.
Johnson, H. L. 1966, *Ann. Rev. Astr. Ap.*, **4**, 193.
Jones, T. J. 1987, in *Late Stages of Stellar Evolution*, ed. S. Kwok and S. R. Pottasch (Dordrecht: Reidel), p. 3.
Joshi, U. C., Deshpande, M. R., Sen, A. K., and Kulshrestha, A. 1987, *Astr. Ap.*, **181**, 31.
Jura, M. 1986, *Ap. J.*, **309**, 732.
Keenan, P. C. 1983, *Bull. Inf. Centre Donnes Stellaires*, **24**, 19.
Keenan, P. C., and Pitts, R. E. 1980, *Ap. J. Suppl.*, **42**, 541.
Kwok, S. 1975, *Ap. J.*, **198**, 583.
———. 1976, *J.R.A.S. Canada*, **70**, 49.
———. 1987, *Phys. Rept.*, **156**, 111.
Kwok, S., and Hrivnak, B. J. 1989, in *Infrared Spectroscopy in Astronomy*, ed. B. Kaldeich (Paris: ESA Pub.), in press.
Kwok, S., Hrivnak, B. J., and Boreiko, R. T. 1987, *Ap. J.*, **321**, 975.
Kwok, S., Hrivnak, B. J., and Milone, E. F. 1986, *Ap. J.*, **303**, 451.
Lamers, H. J. G. L. M., Waters, L. B. F. M., Garmany, C. D., Perez, M. R., and Waelkens, C. 1986, *Astr. Ap.*, **154**, L20.
Likkel, L., Omont, A., Morris, M., and Forveille, T. 1987, *Astr. Ap.*, **173**, L11.
Lub, J., van Paradids, J., Pel, J. W., and Wesselius, P. R. 1979, *Astr. Ap.*, **72**, 82.
Lucas, R., Guilloteau, S., and Omont, A. 1988, *Astr. Ap.*, **194**, 230.
Menzies, J. W., and Whitelock, P. A. 1988, *M.N.R.A.S.*, **233**, 697.
Mutel, R. L., Fix, J. D., Benson, J. M., and Webber, J. C. 1979, *Ap. J.*, **228**, 771.
Nassau, J. J., Stephenson, C. B., and MacConnell, D. J. 1965, *Luminous Stars in the Northern Milky Way VI* (Hamburg: Hamburg Sternwarte and Warner and Swasey Observatory).
Neckel, Th., and Klare, G. 1980, *Astr. Ap. Suppl.*, **42**, 251.
Ney, E. P., and Merrill, K. M. 1980, *Study of Sources in the AFGL Rocket Infrared Study* (AFGL-TR-80-0050).
Nyman, L. A., Johansson, L. E. B., and Booth, R. S. 1986, *Astr. Ap.*, **160**, 352.
Odenwald, S. F. 1986, *Ap. J.*, **307**, 711.
Olofsson, H., Johansson, L. E. B., Hjalmarson, A., and Nguyen-Q-Rieu 1982, *Astr. Ap.*, **107**, 128.
Parthasarathy, M., and Pottasch, S. R. 1986, *Astr. Ap.*, **154**, L16.
Parthasarathy, M., Pottasch, S. R., and Wamsteker, W. 1988, *Astr. Ap.*, **203**, 117.
Pel, J. W. 1976, *Astr. Ap. Suppl.*, **24**, 413.
Percy, J. R., and Welch, D. L. 1981, *Pub. A.S.P.*, **93**, 367.
Pottasch, S. R., and Parthasarathy, M. 1988, *Astr. Ap.*, **192**, 182.
Pottasch, S. R., *et al.* 1984, *Astr. Ap.*, **138**, 10.
Price, S. D., and Murdock, T. L. 1983, *The Revised AFGL Infrared Sky Survey Catalog* (AFGL-TR-83-0161).

Ridgway, S. T., Joyce, R. R., Conners, D., Pipher, J. L., and Dainty, C. 1986, *Ap. J.*, **302**, 662.
Roman, N. G. 1973, in *Spectral Classification and Multicolour Photometry*, ed. Ch. Fehrenbach and B. E. Westerlund (Dordrecht: Reidel), p. 36.
Schönberner, D. 1983, *Ap. J.*, **272**, 708.
Stephenson, C. B., and Sanduleak, N. 1971, *Pub. Warner & Swasey Obs.*, **1**, No. 1.
Thomas, J. A., Robinson, G., and Hyland, A. R. 1976, *M.N.R.A.S.*, **174**, 711.
van Genderen, A. M., van Driel, W., and Greidanus, H. 1986, *Astr. Ap.*, **155**, 72.
Volk, K. M., and Kwok, S. 1987, in *The Late Stages of Stellar Evolution*, ed. S. Kwok and S. R. Pottasch (Dordrecht: Reidel), p. 305.
Volk, K. M., and Kwok, S. 1988, *Ap. J.*, **331**, 435.
———. 1989, *Ap. J.*, **342**, 345.
Wachmann, A. A. 1961, *Astr. Abhand. Hamburger Stern*, **6**, No. 1.
Yamashita, Y., Nariai, K., and Norimoto, Y. 1978, *An Atlas of Representative Stellar Spectra* (New York: Wiley).
Zuckerman, B., and Dyck, H. M. 1986, *Ap. J.*, **311**, 345.
Zuckerman, B., Dyck, H. M., and Claussen, M. J. 1986, *Ap. J.*, **304**, 401.
Zuckerman, B., and Lo, K. Y. 1987, *Astr. Ap.*, **173**, 263.

B. J. HRIVNAK: Department of Physics, Valparaiso University, Valparaiso, IN 46383

S. KWOK: Department of Physics, The University of Calgary, Calgary, Alberta, Canada T2N 1N4

K. M. VOLK: Mail Stop N245-6, NASA Ames Research Center, Moffett Field, CA 94035